AIP | Review of Scientific Instruments

A modified molecular beam instrument for the imaging of radicals interacting with surfaces during plasma processing

Patrick R. McCurdy, K. H. A. Bogart, N. F. Dalleska, and Ellen R. Fisher

Citation: Review of Scientific Instruments **68**, 1684 (1997); doi: 10.1063/1.1147976
View online: http://dx.doi.org/10.1063/1.1147976
View Table of Contents: http://scitation.aip.org/content/aip/journal/rsi/68/4?ver=pdfcov
Published by the AIP Publishing

A modified molecular beam instrument for the imaging of radicals interacting with surfaces during plasma processing

Patrick R. McCurdy, K. H. A. Bogart, N. F. Dalleska,[a] and Ellen R. Fisher[b]
Department of Chemistry, Colorado State University, Fort Collins, Colorado 80523-1872

(Received 4 October 1996; accepted for publication 11 December 1996)

A new instrument employing molecular beam techniques and laser induced fluorescence (LIF) for measuring the reactivity of gas phase radicals at the surface of a depositing film has been designed and characterized. The instrument uses an inductively coupled plasma source to create a molecular beam containing essentially all plasma species. A tunable excimer pumped dye laser is used to excite a single species in this complex molecular beam. LIF signals are imaged onto a gated, intensified charge coupled device (ICCD) to provide spatial resolution. ICCD images depict the fluorescence from molecules both in the molecular beam and scattering from the surface of a depositing film. Data collected with and without a substrate in the path of the molecular beam provide information about the surface reactivity of the species of interest. Here, we report the first measurements using the third generation imaging of radicals interacting with surfaces apparatus. We have measured the surface reactivity of SiH molecules formed in a 100% SiH_4 plasma during deposition of an amorphous hydrogenated silicon film. On a 300 K Si (100) substrate, the reactivity of SiH is near unity. The substrate temperature dependence (300–673 K) of the reactivity is also reported. In addition, reactivity measurements for OH molecules formed in a water plasma are presented. In contrast to the SiH molecule, the reactivity of OH radicals is 0.55 ± 0.05 on the surface of a Si (100) substrate. © *1997 American Institute of Physics.* [S0034-6748(97)00904-0]

I. INTRODUCTION

Understanding the interactions of molecules with surfaces is fundamental to the development of many technologically relevant processes such as chemical vapor deposition (CVD),[1] plasma enhanced CVD (PECVD),[2] plasma etching,[3,4] and surface modification of polymers.[5,6] In all of these processes, chemical and structural changes occur as a result of gas phase molecules interacting with a solid surface. The chemistry associated with these systems is often complicated by the presence of a variety of gas phase species, including radicals, electrons, and ions which can react with each other as well as with the surface being processed. Unfortunately, little is known about gas surface reactions[7,8] within these environments, especially those involving radical species.[9] Yet, radicals are believed to be the most important species in both etching and deposition systems.[10] Indeed, the majority of proposed mechanisms for CVD and PECVD systems cite radicals as the primary film precursors.[3,10,11] Thus, in order to fully understand the chemical mechanisms involved in CVD and PECVD processes, direct measurements of radical surface interactions are needed.

The imaging of radicals interacting with surfaces (IRIS) apparatus described here is designed to measure the surface reactivity of gas phase species during deposition or etching processes.[12–15] This versatile instrument incorporates a differentially pumped vacuum system, spatially resolved laser induced fluorescence (LIF), molecular beams, and rf plasma technology. The IRIS method was first developed nearly a decade ago at Sandia National Laboratories (SNL).[12] The prototype instrument was used to measure the surface reactivity of SiH on a 300 K substrate using a 100% SiH_4 plasma as the molecular beam source. A subsequent instrument at SNL, incorporating differential pumping, has been used to study SiO,[14] NH,[13] and OH radicals.[15] Our third generation IRIS apparatus is greatly improved over the original design by employing a modular design for the vacuum chamber, a heatable substrate, and a state-of-the-art two-dimensional detector.

To demonstrate the capabilities of our new IRIS instrument, we have measured radical surface reactivities in two different systems. In order to compare directly with the original studies, we have measured the reactivity of SiH molecules generated from a 100% silane plasma on a 300 K Si surface. This system deposits amorphous hydrogenated silicon (*a*-Si:H) films which are widely used for photovoltaic converters.[16] Previous measurements of SiH in this system show a surface reactivity near unity.[12] To better characterize the surface interactions of this molecule, we have also measured the surface reactivity as a function of substrate temperature T_s. Dependence of reactivity on substrate temperature was not previously studied for SiH radicals.[12]

The second system studied is the OH radical produced from a 100% H_2O plasma impinging on a 300 K Si substrate. This system neither etches nor deposits a film on the substrate. Previous IRIS results for the same system (using a 300 K oxidized Si_3N_4 substrate) showed a surface reactivity for OH of 0.57 ± 0.05.[15] This experimental system is a good validation for our instrument because it allows the measurement of a radical reactivity that is less than unity. By investigating these two systems with our new IRIS apparatus, we demonstrate that our instrument can accurately measure radical surface reactivities for molecules in very different plasma systems with different surface interactions.

[a]Present address: Nathan Mates, MSC #850, California Institute of Technology, Pasadena, CA 91126-0001.

[b]Author to whom correspondence should be addressed.

 0034-6748/97/68(4)/1684/10/$10.00

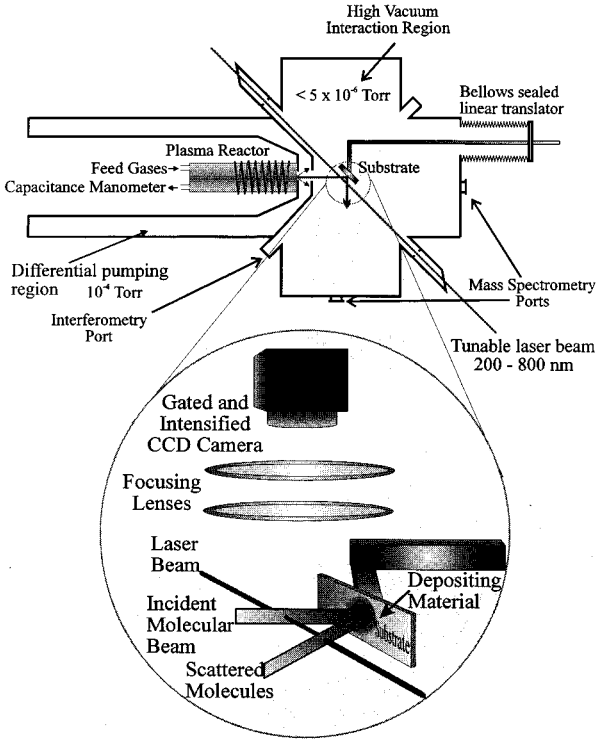

FIG. 1. Schematic of the CSU IRIS apparatus. The detail of the interaction region shows the spatial orientation of the optics and detector relative to the molecular beam and laser beam. The ICCD camera is located perpendicular to the plane of intersection of the laser beam and molecular beam. Specular scattering of the molecules off the substrate is illustrated.

II. INSTRUMENT DESIGN AND PRINCIPLE OF OPERATION

A. Overview

The IRIS apparatus discussed here is based on an experimental design developed at SNL.[12] The original IRIS apparatus had a simple, single chamber design. It operated with a single diffusion pump backed by a mechanical pump for evacuation, and a linear diode array detector for collection of LIF signals. A subsequent design at SNL utilized differential pumping to maintain lower operating pressures in the main chamber. The Colorado State University (CSU) apparatus described here also employs differential pumping, but has the added feature of a gated, intensified charge coupled device (ICCD) camera as the detector.[17] This provides two dimensional images from LIF produced in the region where the laser intersects the molecular beam, hereafter referred to as the interaction region. Additional features have been added to the IRIS experimental design in use at CSU and are described fully below.

A schematic diagram of the IRIS apparatus is shown in Fig. 1. In a typical IRIS experiment, feed gases enter the rear of the plasma tube, rf power is inductively coupled to the gases, and a plasma is produced. Diffusion of the plasma into the differentially pumped region generates a near effusive molecular beam. The molecular beam contains virtually all neutral and ionized species present in the plasma,[13] including the species of interest. After reaching the main chamber, the beam is collimated by a series of slits. A tunable laser beam

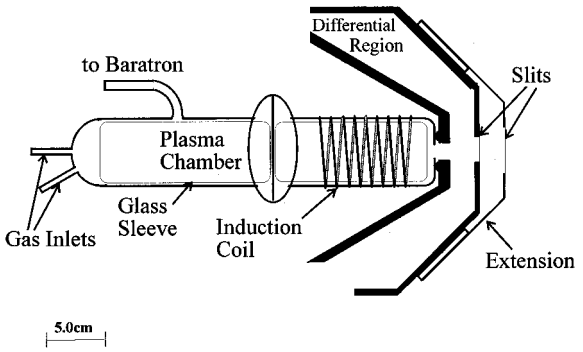

FIG. 2. Enlarged view of the plasma chamber, differential region, and molecular beam formation area. The position of the collimating slit can be varied by ±1 cm by changing the length of the slit extentions.

enters the main chamber and intersects the molecular beam at 45°, exciting the species of interest. Spatially resolved LIF signals are collected by a gated ICCD array. These data correspond to the species of interest in the incident molecular beam. A substrate is then rotated into the path of the molecular beam and spatially resolved LIF is again collected. The substrate is placed at a specified distance, parallel to the laser beam, Fig. 1. Data collected with the substrate in the path of the molecular beam now reflects LIF from incident *and* scattered molecules. The difference between spatial distributions with the surface in and out of the molecular beam is a measure of the radical's surface reactivity. Spatial distributions also indicate scattering mechanisms for radicals investigated (i.e., specular versus adsorption-desorption). State-specific reactivity measurements are made by tuning the laser to absorption frequencies for different rotational states of the radical of interest. Substrates can be heated to determine the substrate temperature dependence of the reactivity and translated away from the laser to characterize the scattered molecules' spatial distribution. Thus, the unique design of the IRIS instrument allows for measurement of the surface reactivity of gas phase species *during* a plasma deposition or etching process. The following sections describe the various components of the IRIS apparatus in detail.

B. Vacuum system and molecular beam formation

The vacuum system comprises three primary regions: (1) the plasma region which is indirectly pumped through the other two regions; (2) the differential pumping region; and (3) the main chamber which includes the interaction region.

(1) Plasma source. The source for the molecular beam is an inductively coupled rf plasma. Figure 2 details the plasma region and the molecular beam formation area of the IRIS apparatus. The plasma chamber is built from two 50 mm i.d. Pyrex glass cylinders with an O-ring joint in the center of the chamber, Fig. 2. The total length of the plasma chamber is 32 cm. Removable glass liners (4.4 cm i.d.) are used in both ends of the plasma reactor to minimize deposition on the inside of the chamber. These liners are replaced periodically when deposits have accumulated on the inside walls.

The pressure in the plasma chamber is monitored using a MKS Baratron capacitance manometer. Base pressure in this region is approximately 1×10^{-6} Torr. Under typical operat-

ing conditions with a 20 sccm flow of argon, pressure in this region is ~0.040 Torr. The source can also be used without a plasma ignited. This would allow the study of surface reactivity during thermal CVD processes. In addition, the plasma housing can be removed and another molecular beam source can be mated to the differential region.

At the back of the plasma chamber there are two 0.635 cm gas inlet ports which are connected to a four line gas manifold. Three of these lines are used for gaseous precursors and gas flow is controlled by MKS mass flow controllers (10–1000 sccm). One of these three lines is dedicated to SiH_4 and Si_2H_6. The fourth line on the manifold is dedicated to high vapor pressure liquids. For liquid precursors, the vapor pressure is controlled by a Nupro bellows sealed metering valve on the gas manifold. The liquid inlet line can be heated from the source bulb to the plasma chamber (typically 45–60 °C).

The front half of the plasma chamber is wrapped with an eight loop induction coil made from 10 gauge nickel plated copper wire, Fig. 2. Radio frequency power (0–300 W, 13.56 MHz) from an ENI HF-300 power supply is inductively coupled to the feed gases through this coil. Coupling is optimized by a rf matching network consisting of an ISI Jennings 100 pF variable capacitor. Typical applied powers are 20–200 W, giving power densities of ~0.088 to 0.88 W/cm^3. A grounded metal screen placed in the chamber confines the plasma to the front 15 cm of the tube. The two halves of the plasma chamber are held together by an aluminum collar that is mounted to the differential pumping region with four long bolts. An O-ring makes a vacuum seal between the plasma chamber and the differential housing. The front end of the glass cylinder contains a 1.0 cm diameter orifice through which gas molecules diffuse into the differential region.

(2) Differential region. A molecular beam is formed as species diffuse from the 1.0 cm hole in the plasma chamber through a 1.27 cm hole in the differential housing and into the differential pumping region, Fig. 2. This region has a volume of ~19 ℓ and consists of the space between the plasma housing and the main chamber. The differential region is pumped by a 4,200 ℓs^{-1} Varian HS-10 diffusion pump, backed by a Leybold D30A mechanical pump (12.6 ℓs^{-1}) and equipped with a manually operated gate valve located between the pump and the chamber. The differential region reaches a base pressure of 1×10^{-7} Torr when pumped overnight, as measured with a Granville–Phillips hot ionization gauge. The typical operating pressure in this chamber, measured during an IRIS experiment (e.g., 20 sccm Ar or 10 sccm SiH_4 flow) is $\sim 2.5 \times 10^{-4}$ Torr.

The differential region and the main chamber are separated by a wall 25 mm from the end of the plasma chamber, Fig. 2. The differential wall is ~3.1 mm thick and contains a 2.5 cm diameter hole, directly in line with the hole in the end of the plasma chamber. The size of this orifice can easily be decreased by mounting a defining slit on the main chamber side of the wall. The plasma molecular beam species diffuse through this hole and into the main chamber.

3. Main chamber. The main chamber is the largest chamber of the IRIS apparatus, with a volume of ~32 ℓ. It is pumped by a 4200 ℓs^{-1} Varian HS-10 diffusion pump backed by a Welch 1397 mechanical pump (8.3 ℓs^{-1}) and equipped with a water baffle and pneumatic gate valve stacked between the pump and the chamber. This chamber reaches a base pressure of 1×10^{-7} Torr after pumping overnight, as measured by a Granville–Phillips hot ionization gauge. The typical operating pressure in the main chamber (with two defining slits, ~1.0 mm each) during an IRIS experiment (e.g., 20 sccm Ar or 10 sccm SiH_4) is $\sim 4 \times 10^{-6}$ Torr.

Under normal experimental conditions, the vast majority of the plasma molecular beam species are pumped away in the differential region and do not enter the main chamber. The remaining particles diffuse through a series of defining slits, Fig. 2, forming a well-collimated molecular beam. Two slits are usually used to define the molecular beam spatially. The first defining slit (typically ~1 mm wide and 19 mm long) is mounted directly on the main chamber side of the differential wall, ~31 mm from the plasma tube. The molecular beam is then further collimated by a second slit usually mounted on stainless steel extensions attached to the differential wall, Fig. 2. With these extensions, the minimum distance between the differential wall and the second defining slit is ~10 mm. This distance can be increased up to ~25 mm. With our experimental design, however, it is not necessary to mount the second slit on the extensions. This allows for maximum flexibility in beam formation. The width of the second slit can also be varied, but is usually 0.8–1.25 mm wide and 19 mm long. For the SiH experiments, the second slit was located 10 mm from the differential wall and 26 mm from the interaction region. For the OH experiments, the second slit was placed 10 mm from the differential wall and 36 mm from the interaction region. Additional slits may also be used for further collimation.

The use of a rectangular molecular beam rather than a circular beam has two advantages. First, for beams of equivalent fluxes, a rectangular beam provides higher spatial resolution in the horizontal direction. Second, this configuration increases the detection sensitivity to molecules scattered/desorbed from the surface because molecules emanating from a line source decrease in density as $1/r$ rather than the $1/r^2$ resulting from a point source.

C. Substrate control

The design of the IRIS apparatus allows for use of a variety of substrate types and sizes that can be mounted on one of two holders. The first substrate holder consists of a 2.5 cm aluminum rod machined at a 45° angle. The machined surface is an ellipse, measuring ~2.5×3.6 cm on its surface. The substrate is affixed directly to this surface either by Apiezon Wax W or double sided cellophane tape. The base of the aluminum rod has also been machined with a hole large enough to accommodate the manipulator arm rod.

The second substrate holder used in IRIS experiments has a more complicated design, Fig. 3. This holder starts with the basic design of the simpler substrate holder, a base made from a 2.5 cm aluminum rod machined at a 45° angle. A rectangular aluminum base plate (2.54 cm×5.08 cm) is positioned above the machined surface of the base, thermally

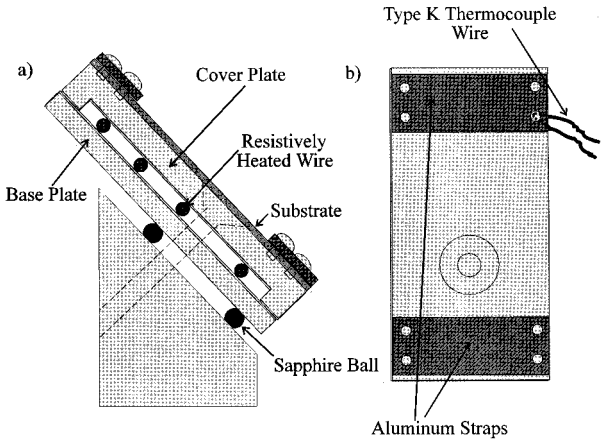

FIG. 3. Detail of the heatable substrate holder (a) side view and (b) top view. Samples are held onto the head by means of the two aluminum straps. The thermocouple is held in contact with the substrate by placing it under the strap held by the set screws.

isolated by three sapphire balls (3.2 mm diameter). Sandwiched between the base plate and the cover plate (2.54 cm $\times$5.08 cm) is a $\sim$15 cm long S-shaped nichrome wire, Fig. 3. The nichrome wire is electrically isolated with a MgO layer enclosed in Inconel casing. The cover plate, base plate, and base are held together by a 19 mm long machine screw. Substrates are mounted on the cover plate by means of two aluminum straps (2.54$\times$0.95 cm) located on each end of the cover plate.

Both substrate holders can be mounted on an L-shaped manipulator arm attached to a Vacuum Generator Ltd. bellows seal, linear motion feedthrough with a 10 cm translation capability, Fig. 1. The arm allows the substrate to be rotated precisely in and out of the path of the molecular beam and to be translated away from the interaction region. Translation of the substrate effectively varies the laser-surface distance. Typically, the substrate is positioned such that it is 2.0 to 5.0 mm from the laser beam.

Using the heatable substrate holder, the temperature of the substrate can be controlled from ambient temperature ($\sim$300 K) to $\sim$750 K using an Omega CN9000A temperature controller with a *K*-type thermocouple wire. A Kepco ATE 6-25M power supply (6 V, 25 A) resistively heats the surface by passing current through the nichrome wire located between the cover plate and the base plate of the holder. The thermocouple wire is positioned under one of the aluminum straps on the holder, physically in contact with the front of the substrate, Fig. 3. The temperature is monitored with the Omega controller. Small ($\sim$1.5$\times$5 cm) pieces of Si (100) wafers were used as substrates for all experiments described here. These substrates were cleaned with methanol prior to mounting on a substrate holder. No additional cleaning was done to remove the 30–80 Å of native oxide.

D. Laser system

Monochromatic light at the desired excitation wavelength is produced with an excimer pumped dye laser system. The Lambda Physik LPX 110i excimer laser (XeCl) emits 308 nm pulsed light with a pulse width of 17 ns at FWHM. The pump laser is typically operated with a pulse energy of 80–150 mJ at a repetition rate of 100 Hz. The pulse energy can be adjusted to saturate the LIF signal, thus minimizing the problem of laser output power fluctuations. The excimer laser pumps a Lambda Physik Scanmate 2 dye laser in order to produce tunable light. Using the appropriate dye, output wavelengths can be scanned from 330 nm to above 1036 nm. In addition, our system can access wavelengths between 205 and 330 nm with the addition of either a KDP or a BBO doubling crystal. Pulse-to-pulse energy measurements can be made on the laser beam either before entering the chamber, after exiting the chamber or both simultaneously using a Molectron JD2000 joulemeter ratiometer with the appropriate head(s).

In the SiH system, light in the 409–415 nm range was produced using Furan-2 in the dye laser. The measured output power from the dye laser was 3–6 mJ per pulse (100 mJ pump energy). For the OH data, light in the 306–310 nm range was produced using Rhodamine B in the dye laser and frequency doubling the output with a KDP crystal. The measured output power of the double light was 180–750 μJ per pulse (80–100 mJ pump energy).

The output of the dye laser is directed into the main chamber of the IRIS apparatus via a prism, a focusing lens, and a periscope. The laser beam enters the interaction region through a Brewster angle window, parallel to the substrate at a 45° angle from the molecular beam, Fig. 1. Two different optical arrangements were used in these experiments. For the SiH measurements, the laser beam also passed through a $\sim$1 mm diameter aperture 12 cm before the interaction region to reduce scattered light in the chamber. The focusing lens was a 50.8 mm diameter synthetic fused silica plano-convex lens (f=2000 mm) placed outside the chamber, $\sim$2200 mm from the interaction region. This produced a focal point prior to the interaction region, and gave a well-defined laser beam, $<$1 mm wide at the intersection of the molecular beam and the laser.

For the OH experiments, the laser beam was focused with a shorter focal length lens (f=630.1 mm) placed 760 mm from the interaction region. This gave a laser beam width of $<$1.0 mm at the interaction region. Two apertures were used to aid in definition and alignment of the laser beam. A 1.95 mm aperture, placed 180 mm from the interaction region, was used to better define the laser beam shape and reduce scattered light in the chamber. A 2.10 mm aperture, placed 180 mm after the interaction region, was used to align the laser through the chamber. A third optical arrangement with two focusing lenses in series can also be used to give a well-defined, collimated laser beam at the interaction region.

E. Fluorescence detection

The spatial dependence of the fluorescence excited by the laser beam is measured by imaging light from the interaction region on a Princeton Instruments (PI) gated ICCD camera. The camera is equipped with a microchannel plate image intensifier and both uv and ir enhancement coatings. The ICCD camera is electrothermally cooled to an operating range of -22 to -40 °C. The high gain of the microchannel

plate and the low readout noise of the ICCD array result in a very sensitive detector capable of responding to a single photon. The ICCD has a 586×384 pixel display, corresponding to an area of 109 mm^2. For IRIS experiments, the detector is oriented with its long axis along the laser beam.

For fluorescence excitation spectra and reactivity experiments, the fluorescence is imaged directly onto the ICCD array, Fig. 1. The light is collected with two 50 mm diameter synthetic fused silica lenses. One lens ($f=300$ mm) collects and collimates the light above the interaction region. The second lens ($f=75$ mm) then focuses the fluorescence onto the ICCD array, Fig. 1. The optics demagnify the image so that the 12.9 mm long array views a region 55.0 mm long, making it possible to spatially resolve both the incident and scattered beam simultaneously. The total area imaged by the ICCD array is 1980 mm^2. Bandpass filters can be used between the chamber and the lenses to reduce spurious signal due to scattered light from the laser or plasma source. Indeed, in the SiH substrate temperature dependence studies, an IR cutoff filter (>800 nm) was used to eliminate light noise from the heated Si substrate. In the OH system, a 340 nm cutoff filter was used to minimize signal from plasma emission.

The ICCD is located perpendicular to both the molecular beam and the laser beam, directly above the interaction region, Fig. 1. Typically, the ICCD is gated on 1.1 μs after the laser fires, to avoid interference from scattered laser light. The gate width is varied according to the fluorescence lifetime of the species of interest. The radiative lifetimes of SiH and OH are fairly similar, 534 ns[18] and 688±7 ns,[19] respectively. For both molecules, a 1.0 μs gate width was used to collect the fluorescence. During all IRIS experiments, signals are generally collected for 10–100 accumulations. An accumulation is typically 2–60 s long with the laser firing at 100 Hz. Fewer accumulations decrease readout noise. For the SiH experiments described here, 10 accumulations of 20 s each were used with the laser firing at 100 Hz. For the OH experiments, 10 accumulations of 10 s each were used. Pixel binning (typically 4×4 groups) is used to realize signal-to-noise ratio enhancement and minimize data collection time.

F. System integration

Figure 4 shows a schematic of the electronics configuration for the collection of reactivity data with the IRIS apparatus (dashed lines). The computer is a 486 DX 33 MHz with 20 megabytes of RAM using PI Win View software, linked to the ICCD camera via a PI ST-130 detector controller. The controller is connected through its notscan output to a PI PG-200 programmable pulse generator (''notinhibit'' in). Since fluorescence from multiple laser pulses are accumulated on the ICCD-during the IRIS experiment, the controller sends a notscan signal to the pulse generator during image readout. The PG-200 in turn sends the trigger signal (trigger out) to the laser to initiate firing (trigger in). An oscilloscope is connected to the PG-200 to monitor the signal from the PG-200 to the laser.

The electronics configuration is slightly different when collecting an excitation spectrum for the species of interest in an IRIS experiment, Fig. 4 (solid lines). The main difference between the configurations shown in Fig. 4 is that the laser now triggers the PG-200, rather than the PG-200 triggering the laser. This allows the laser to control the ICCD camera. The ST-130 sends a feedback signal to the dye laser to change the grating position. The ST-130 output signal is shortened by an HP pulse generator so the signal can be recognized by the laser.

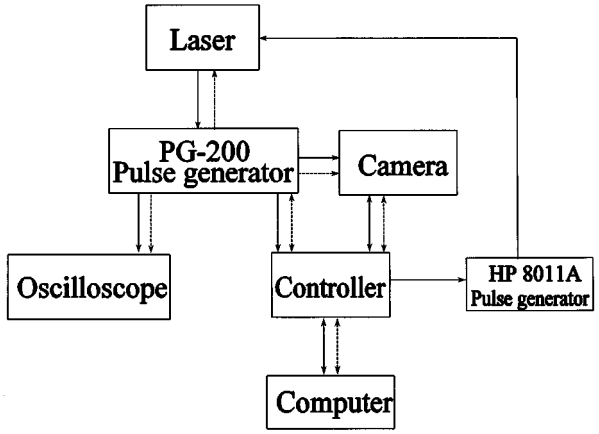

FIG. 4. Schematic of the electronics configuration for collection of IRIS reactivity data (dashed lines) and for collection of rotational excitation spectra (solid lines).

G. Additional features

The IRIS instrument at CSU has a number of features that have been added to the basic design employed at SNL. First, the apparatus has two ports which can accommodate a mass spectrometer, Fig. 1. These ports are located at the rear of the main chamber, to accommodate an in-line mass spectrometer and on the side of the main chamber, perpendicular to the molecular beam axis. The latter configuration would be employed to monitor molecules desorbing from the substrate. Addition of a mass spectrometer to IRIS will provide information on gas phase species present in the molecular beam, and may be used to detect species scattered off the substrate.

A second feature is an additional set of laser ports located 90° from the laser ports used in a typical IRIS experiment. As noted in Fig. 1, the port located perpendicular to the substrate surface can be used for laser interferometry on the depositing film. This would allow us to determine *in situ* film deposition rates during processing. This port may also be adapted for Raman or Fourier transform infrared spectroscopy, allowing for additional *in situ* surface characterization.

Other features include: a nitrogen purge, allowing for greatly reduced pump down times after the chamber is vented for short periods; a power-pressure-water interlock system that triggers the shut down of the pumping system in case of increased chamber pressure, power failure, or decreased water flow; and inlet and vent ports for liquid nitrogen feedthroughs for cooled molecular beam slits.[13]

III. RESULTS AND PERFORMANCE

Ho, Breiland, and Buss (HBB) first used the IRIS technique to study SiH radicals from a 100% SiH_4 plasma on a

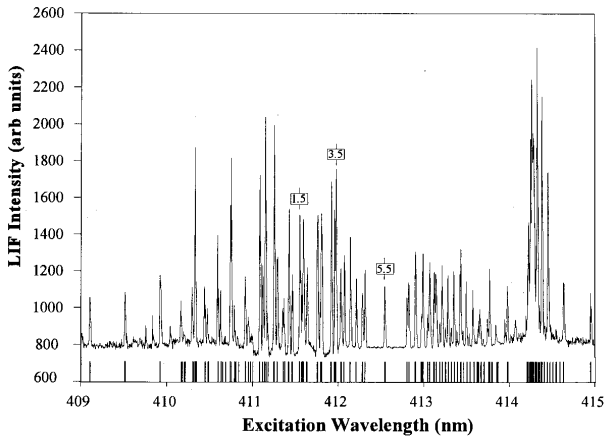

FIG. 5. Experimental fluorescence excitation spectrum of SiH in the molecular beam formed from a 100% SiH_4 plasma. The lines labeled [1.5], [3.5], and [5.5] are the $R_{21}(J=1.5), Q_{21}(J=3.5), R_{22}(J=5.5)$ rotational lines used in this study. Plotted below the experimental spectrum are the calculated line positions for the SiH rotational states.

300 K Si substrate.[12] Substrate temperature dependence measurements, however, were not performed in the original experiments. Here, we present results for SiH radicals from a 100% SiH_4 plasma on 300 K Si substrates to test the performance of our apparatus. In addition, we present results for the substrate temperature dependence (300–673 K) of SiH molecules at the surface of a depositing *a*-Si:H film. As a further demonstration of our instrument's capabilities, results for OH molecules produced in a 100% H_2O plasma are also shown.

A. Spectroscopy of SiH

The spectral selectivity of the LIF technique was used to identify and study SiH separately from the other species in the molecular beam. Figure 5 shows an experimental fluorescence excitation spectrum for SiH obtained with laser wavelengths between 409 and 415 nm. Also shown in Fig. 5 are the calculated[20] line positions from a numerical simulation of the well-known spectroscopy of the SiH $A^2\Delta - X^2\Pi$ transition.[20–23] The experimental spectrum is not corrected for variations in laser power and was obtained using a broader molecular beam than was used for the reactivity measurements in order to improve the signal levels. The good agreement between the calculated line positions and experimental spectra shows the fluorescing species is indeed SiH.

The IRIS method for measuring radical reactivities is not adversely affected by optical saturation because the signal from desorbing molecules is normalized to the signal from the incident molecular beam. All IRIS measurements reported here were performed under optically saturated conditions. Since we are only concerned about the ratio of incoming molecules to scattered molecules in a steady state, measurements are unaffected by operating in a saturated regime. Saturation effects in IRIS experiments have been discussed in detail previously.[12,15]

B. Spatial dependence of SiH

The ICCD camera allows two-dimensional imaging of LIF from SiH molecules. Figure 6 displays the images obtained for SiH using a 100% SiH_4 plasma as the molecular beam source. These images have been corrected for background signal from scattered laser light and plasma emission with no additional manipulations. In Fig. 6, the laser is propagating from the bottom of the image to the top and the molecular beam is propagating from left to right across the image. The laser was tuned to 411.546 nm, which excites the R_{21} ($J=1.5$) state of SiH. Figure 6(a) shows an image of LIF from SiH in the molecular beam as it intersects the laser beam. Figure 6(b) shows the fluorescence with the Si substrate (300 K) rotated into the path of the molecular beam, 2.5 mm from the laser beam. This signal corresponds to SiH molecules both in the incident molecular beam and scattering off the surface of a depositing *a*-Si:H film. The difference between Figs. 6(b) and 6(a) is shown in Fig. 6(c), corresponding to SiH molecules emanating from the substrate. From this figure, it is clear very little SiH is scattering off the depositing film. The physical location of the SiH molecules is given by the images in Fig. 6.

To directly compare with previous IRIS results for SiH from a SiH_4 plasma, we have taken vertical cross-sections of the image data shown in Fig. 6. Combining the signals for a 1.16 mm wide strip along the laser beam for each image in Fig. 6 results in the three curves shown in Fig. 7. The LIF signal from molecules in the incident molecular beam is nearly identical to the LIF signal taken with the substrate in the path of the molecular beam. This indicates there is very little, if any, scatter from the substrate. The data in Fig. 7 are very similar to those produced with the original IRIS apparatus equipped with a linear diode array.[12]

The observation that signals from the scattered/desorbed SiH molecules are only a few percent of the signals from the SiH in the molecular beam suggests that most of the SiH molecules react at the surface. The reactivity R of a particular radical with a substrate is defined in Eq. (1),

$$R = 1 - \frac{F_{\text{scat}}}{F_{\text{mb}}}, \tag{1}$$

where F_{scat} is the flux of molecules emanating from the surface and F_{mb} is the flux of incoming molecules. Hence, the reactivity can be considered as the probability that a radical will disappear from the gas phase as a result of its interaction with the substrate. HBB measured a high reactivity of 0.94 on a room temperature Si substrate.[12] Our data indicate a reactivity of 0.95 ± 0.05 for SiH molecules at the surface of a depositing *a*-Si:H film, in excellent agreement with HBB.

C. Temperature dependence of SiH

Industrial scale deposition of *a*-Si:H films is normally performed at substrate temperatures well above 300 K.[11] It is imperative, therefore, to measure radical reactivities at elevated substrate temperatures in order to achieve full understanding of these processes. The previous SiH reactivity measurements were performed only on 300 K substrates. Published reactivity values for the OH molecule on a heated substrate show a clear temperature dependence,[15] suggesting that substrate temperature T_s may affect the reactivity of SiH

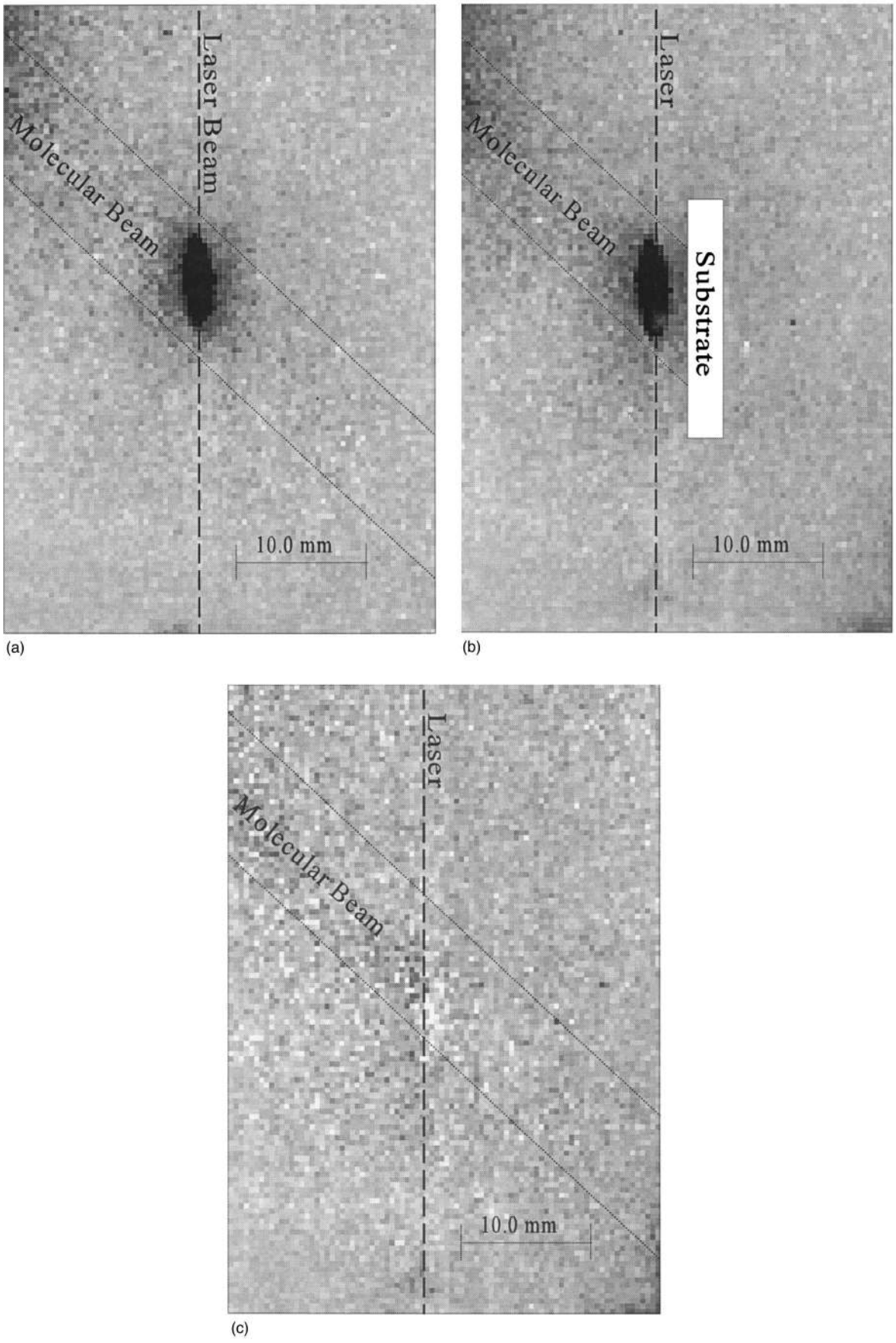

FIG. 6. ICCD images of LIF signals produced by SiH molecules (a) in the molecular beam only (no substrate) and (b) with the substrate in the path of the molecular beam, 2.5 mm from the laser. The image shown in Figure (c) is the difference between images (a) and (b), corresponding to SiH molecules scattering from the substrate. The dashed lines indicate the location of the molecular beam and the laser beam in the images. LIF signals with the highest intensity appear as the darkest regions in the image. A sum of four data sets is shown.

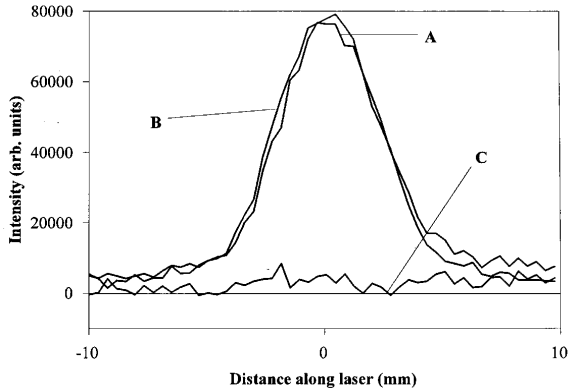

FIG. 7. Cross-sectional data from the images shown in Fig. 6. The y axis is the signal intensity of a 1.16 mm swath centered along the laser beam path. The x axis corresponds to the distance along the laser beam, where the zero point corresponds to the intersection of the laser and the molecular beam. The three curves correspond to LIF signals for SiH observed in the incident molecular beam (A), with the substrate in the path of the molecular beam (B), and for SiH desorbing from the surface (C).

molecules. Therefore, we have examined the effects of T_s on surface reactivity of SiH as a further demonstration of our instrument's capabilities.

We have measured the surface reactivity of SiH at T_s=300, 373, 473, 573, and 673 K for three rotational states, J=1.5, 3.5, and 5.5. Figure 8 shows one example of LIF signals using the J=3.5 rotational state at T_s=673 K. There is no discernable difference between this figure and the data collected as shown in Fig. 7. Thus, at elevated substrate temperatures and with different rotational states, signal from scattered SiH is negligible. This is true for all substrate temperatures and all rotational states studied.

D. Spectroscopy of OH

Using a 100% water plasma, the OH radical was spectroscopically isolated, identified, and studied with LIF. A well-defined molecular beam was used during collection of the OH excitation spectrum generated by tuning the laser system from 307 to 309.5 nm, Fig. 9. No corrections for fluctuations in laser power were made. A comparison of the experimental spectral line positions with a calculated OH

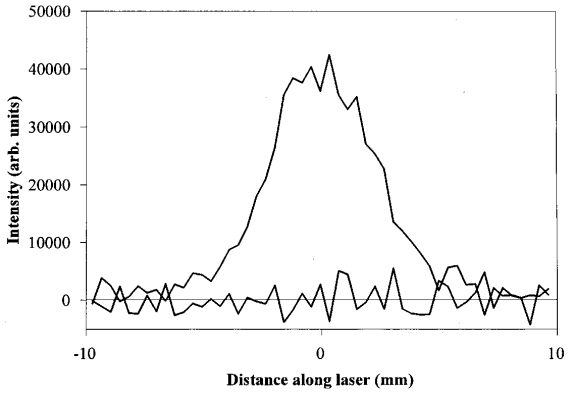

FIG. 8. LIF signals for SiH in the molecular beam (upper trace) and scattered from the substrate (lower trace) using elevated substrate temperatures (T_s=673) and alternate rotational states (J=3.5).

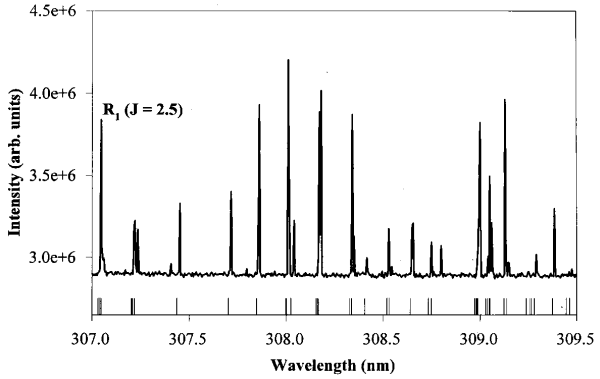

FIG. 9. Experimental fluorescence excitation spectrum of OH in the molecular beam formed from a 100% water plasma. The labeled line is the $R_1(J=2.5)$ (λ_{ex}=307.050 nm) rotational state of OH. Below the experimental spectrum is a plot of calculated line positions for OH.

excitation spectrum for the $A\ ^2\Sigma^+ - X\ ^2\Pi(0,0)$ transition band,[24] Fig. 9, verifies that the fluorescing species is clearly OH.

E. Spatial dependence of OH

As noted above, a moderate surface reactivity for OH molecules has previously been determined using the IRIS technique.[15] This measurement was made using a low power, low pressure 100% H_2O plasma impinging on a silicon nitride substrate. In order to compare directly to these previous OH reactivity results, vertical cross sections were generated from LIF images for the $R_1(2.5)$ rotational state (λ=307.050 nm) of OH generated from a 100% H_2O plasma, Fig. 10. These curves are the result of combining the signals for a 5.42 mm wide strip along the laser beam. In contrast to the SiH molecules, it is clear from this figure that a significant fraction of the OH molecules are coming off the surface. As with the SiH data, the LIF signals shown in Fig. 10 are directly related to the spatial distributions of the OH molecules. Since the incident molecular beam impinges on the substrate at a 45° angle, signal from scattered molecules

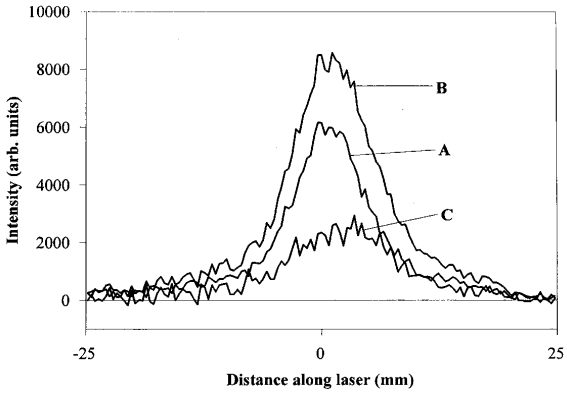

FIG. 10. Cross-sectional data of LIF produced by OH radicals using a H_2O plasma molecular beam. The y axis is the signal intensity of a 5.4 mm swath centered along the laser beam. The x axis is the distance along the laser beam, with the zero point corresponding to the intersection of the laser and the molecular beam. The three curves correspond to LIF signals for OH observed in the incident molecular beam (A), with the substrate in the path of the molecular beam (B), and for OH desorbing from the surface (C). An average of five data sets is shown.

should appear in a different location on the ICCD array. In addition, the scattered molecules will have a different spatial distribution than the incident molecules. Both of these effects can be seen in Fig. 10. The scattered signal is shifted along the laser beam by 1.7 ± 0.2 mm. This is in reasonable agreement with the predicted value of 2 mm.[25] In addition, the scattered signal has a broader angular distribution than that of the incident molecular beam. These two observations imply the OH molecules are scattering with a cosine distribution (adsorption/desorption mechanism).

We can further compare our results to those previously published by quantitatively modeling the signals due to molecules in the incident molecular beam and scattering from the surface. A detailed description of our geometric model is given elsewhere.[26] Our simulations of the data indicate 45% of the molecules are scattering from the surface. This indicates a reactivity of 0.55 ± 0.10 for OH in a H_2O plasma molecular beam incident on a SiO_2 substrate. This agrees well with the previous measurements of $R=0.57\pm0.05$ for OH on an oxidized Si_3N_4 substrate.[15]

IV. DISCUSSION

The multitude of gas-surface interactions that occur during plasma processing is difficult to characterize precisely. During PECVD, the growing film surface is continuously bombarded with reactive neutral molecules, ions, and high energy photons, yielding a complex steady state surface composition. The resulting film chemistry, morphology, electronic and structural properties for any system are directly affected by the interactions of these reactive species with the substrate. Indeed, radicals are believed to be the most important species in many plasma etching and deposition systems.[10] Thus, it is desirable to know how the individual plasma species interact at the surface of the material being processed. The IRIS technique allows the study of one specific molecule interacting at a surface while the surface is being processed by the full range of plasma species.

A. SiH radicals

The new IRIS apparatus described here has been used to study the rotational state resolved reaction of SiH with the surface of *a*-Si:H during plasma deposition and of OH with the surface of a Si substrate. With SiH, we measure a surface reactivity of 0.95 ± 0.05 on a room temperature substrate, in good agreement with previous IRIS measurements.[12] Furthermore, the reactivity does not change measurably with substrate temperature from 300 to 673 K. This high reactivity of SiH radicals on the surface of a depositing *a*-Si:H film suggests that SiH may be an important species in the deposition process. Note, however, that these experiments simply measure the disappearance of SiH molecules from the gas phase, but do not distinguish between loss mechanisms on the surface. That is, there is no distinction between SiH molecules that are incorporated into the depositing film and SiH molecules that undergo a surface reaction to form another species that desorbs from the surface [e.g., $SiH(ads)+H(ads)\rightarrow SiH_2(g)$]. It is possible, however, that SiH formed under different conditions and plasma exposure may exhibit a different reactivity than that observed here.[27]

There is extensive debate in the literature over the importance of various precursors in PECVD of *a*-Si:H from SiH_4 plasmas. As IRIS data can aid in understanding the roles of various precursors to deposition processes, a brief discussion of this debate is warranted here. Much of the discussion has centered on the role of the various radicals present in these systems, specifically SiH_x ($x=1$–3). Most researchers agree that SiH_3 is the most important precursor under typical deposition conditions. This is based primarily on experimental evidence that SiH_3 is the dominant monosilicon radical in SiH_4 plasmas.[28,29] In addition, several studies on the gas phase reactions of SiH_x radicals show that SiH and SiH_2 react rapidly with SiH_4 (the dominant species in typical rf SiH_4 plasmas[7]), while SiH_3 does not.[30–33] SiH_3 does, however, react very rapidly with other radicals.[7] This leads to a long lifetime for SiH_3 radicals in a silane plasma. Doughty and Gallagher have shown that SiH_x species are produced primarily in the center of an rf discharge, away from the substrate.[34] For these radicals to contribute to film growth, they must travel some distance to reach the substrate. Thus, a long lifetime is crucial for them to have a significant role in film growth. This suggests that even if SiH and SiH_2 have significant concentrations in the center of the plasma, they will not reach the film surface in ample numbers to be important in film deposition.[34]

In addition to the number densities of the various possible film precursors, we must also consider their surface reactivities. Here, we have shown the surface reactivity of SiH is near unity at the surface of a depositing *a*-Si:H film using $T_s=300$–673 K. IRIS measurements are the only direct measurement of a surface loss coefficient β for SiH_x radicals currently available. Other literature studies have estimated β for SiH_2 and SiH_3 radicals. Values for SiH_3 range from 0.050 on a hydrogenated, chlorinated silicon surface,[35] to 0.2 on *a*-Si:H.[36] In addition, Perrin and Broekhuizen estimate that $\geqslant 60\%$ of adsorbed SiH_3 recombine with other radicals at the surface and desorb.[36] Some researchers believe, however, that a low surface loss coefficient leads to greater surface mobility for film precursors which ultimately leads to a better quality material.[37] The only β value available for SiH_2 comes from Robertson and Rossi who measured $\beta(SiH_2)=0.15$ on an *a*-Si:H film.[38] Hence, although the number density of SiH radicals in SiH_4 plasmas is considerably less than that of SiH_3, the considerable difference in β values of these molecules implies that SiH could be an important precursor, depending on the plasma parameters.

Another factor that must be considered in determining the relative importance of SiH_x radicals to film growth is the specific plasma conditions used to deposit *a*-Si:H. Several studies show that increasing plasma power decreases the number density of SiH_4 while increasing the number density of other plasma species.[39–41] In addition, Perrin and coworkers have determined there are two deposition regimes in SiH_4 plasmas, the α regime and the γ regime.[42] The γ regime can be accessed by either high pressures or high electrode bias voltages and is characterized by an increased electron density.[43] In this regime, there is an increase in the relative number density of SiH_x radicals in the plasma.[41,42] In our IRIS experiments, we observe a higher number density of

SiH molecules when the plasma source is operating at pressures above 20 mTorr. This would imply that in the γ regime, SiH radicals could be important contributors to film growth.

The IRIS data presented here for the SiH molecule is not meant to provide the final word in the debate over the most important precursors for a-Si:H deposition. Rather, we hope to provide further insight into the mechanisms for a-Si:H deposition by performing IRIS experiments on other radicals present in SiH_4 based systems. By developing a more complete picture of the interactions of radicals with surfaces during deposition of a-Si:H films, we can draw better conclusions about the role of silicon hydride species in film growth.

B. OH radicals

In the OH experiments, we do not observe either film deposition or etching of the Si substrates. FTIR analysis of a substrate after exposure to the H_2O plasma molecular beam showed adsorbed OH and minor hydrocarbon contaminants.[44] Therefore, in our experiments, OH is reacting at a surface that should be primarily covered with silanol groups. In this system, we measure a surface reactivity of 0.55 ± 0.05 on a 300 K substrate.[45] This moderate reactivity was seen previously,[15] and the loss mechanism for OH was attributed to hydrogen abstraction from either an isolated silanol group or with hydrogen bonded pairs of surface silanol groups to give water. The overall observed effect is the recombination of OH with other species from the molecular beam or on the surface. However, no net reaction occurs with the underlying substrate at steady state. This is supported by the observation that exposure to the H_2O plasma does not significantly deposit material or etch the substrate. Further characterization of the surface reactivity of OH molecules under SiO_2 film deposition conditions is currently underway.[26]

ACKNOWLEDGMENTS

Support for this research comes from the Office of Naval Research and Sandia National Laboratories. The authors also acknowledge support from Colorado State University through the Faculty Diversity Career Enhancement Fund and Faculty Research Grants program.

[1] K. E. Spear and J. Carlson, Electrochem. Soc. Interface **2**, 39 (1993).
[2] R. Reif and W. Kern, *Thin Film Processes II*, edited by J. L. Vossen and W. Kern (Academic, San Diego, CA, 1991), p. 525.
[3] M. A. Lieberman and A. J. Lichtenberg, *Principles of Plasma Discharges and Materials Processing* (Wiley, New York, 1994).
[4] H. W. Lehmann, *Thin Film Processes II*, edited by J. L. Vossen and W. Kern (Academic, San Diego, CA, 1991), p. 673.
[5] F. D. Egitto and L. J. Matienzo, IBM J. Res. Dev. **38**, 423 (1994).
[6] N. Morosoff, *Plasma Deposition, Treatment, and Etching of Polymers*, edited by R. d'Agostino (Academic, New York, 1990) p. 528.
[7] J. M. Jasinski and S. M. Gates, Acc. Chem. Res. **24**, 9 (1991).
[8] M. Masi, B. Giambattista, L. Canzi, and S. Carra, Chem. Eng. Sci. **49**, 669 (1994).
[9] We follow Herzberg's example and use the term ''radical'' to refer to transient intermediate species, rather than limiting the term to only those species with an unpaired electron. G. Herzberg, *The Spectra and Structures of Simple Free Radicals* (Cornell University, Ithaca, NY, 1971).
[10] R. d'Agostino, *Plasma Deposition, Treatment, and Etching of Polymers*, edited by R. d'Agostino (Academic, San Diego, CA, 1990), p. 528.
[11] G. Bruno, P. Capezzuto, and G. Cicala, *Plasma Deposition of Amorphous Silicon-Based Materials*, edited by G. Bruno, P. Capezzuto, and A. Madan (Academic, Boston, 1995), p. 27.
[12] P. Ho, W. G. Breiland, and R. J. Buss, J. Chem. Phys. **91**, 2627 (1989).
[13] E. R. Fisher, P. Ho, W. G. Breiland, and R. J. Buss, J. Phys. Chem. **96**, 9855 (1992).
[14] R. J. Buss, P. Ho, and M. E. Weber, Plasma Chem. Plasma Process. **13**, 61 (1993).
[15] E. R. Fisher, P. Ho, W. G. Breiland, and R. J. Buss, J. Phys. Chem. **97**, 10 287 (1993).
[16] A. Madan, *Plasma Deposition of Amorphous Silicon-Based Materials*, edited by G. Bruno, P. Capezzuto, and A. Madan (Academic, San Diego, CA, 1995), p. 243.
[17] The IRIS apparatus currently in use at SNL now also employs an ICCD. R. J. Buss and P. Ho, IEEE Trans. Plasma Sci. **24**, 79 (1996).
[18] H. Bauer, K. H. Becker, R. Duren, C. Hubrich, and R. Meuser, Chem. Phys. Lett. **108**, 560 (1984).
[19] K. R. German, J. Chem. Phys. **62**, 2584 (1975).
[20] L. Klynning and B. Lindgren, Ark. Fys. **33**, 73 (1966).
[21] A. E. Douglas, Can. J. Phys. **35**, 71 (1957).
[22] C. V. Jackson, Proc. R. Soc. London, Ser. A **126**, 373 (1930).
[23] J. Perrin and E. Delafosse, J. Phys. D **13**, 759 (1980).
[24] J. A. Coxon, Can. J. Phys. **58**, 933 (1980).
[25] This value is predicted from the geometry of the experiment using a laser-surface distance of 2 mm, assuming an adsorption/desorption mechanism.
[26] K. H. A. Bogart, J. P. Cushing, and E. R. Fisher (unpublished).
[27] G. R. Barker, P. R. McCurdy, and E. R. Fisher (unpublished).
[28] R. Robertson and A. Gallagher, J. Appl. Phys. **59**, 3402 (1986).
[29] N. Itabashi, N. Nishiwaki, M. Magane, T. Goto, A. Matsuda, C. Yamada, and E. Hirota, Jpn. J. Appl. Phys. **29**, 585 (1990).
[30] J. P. M. Schmitt, P. Gressier, M. Krishnan, G. De Rosny, and J. Perrin, Chem. Phys. **84**, 281 (1984).
[31] M. H. Begemann, R. W. Dreyfus, and J. M. Jasinski, Chem. Phys. Lett. **155**, 351 (1989).
[32] G. Inoue and M. Suzuki, Chem. Phys. Lett. **122**, 361 (1985).
[33] J. M. Jasinski and J. O. Chu, J. Chem. Phys. **88**, 1678 (1988).
[34] D. A. Doughty and A. Gallagher, J. Appl. Phys. **67**, 145 (1990).
[35] J. M. Jasinski, J. Phys. Chem. **97**, 7385 (1993).
[36] J. Perrin and T. Broekhuizen, Appl. Phys. Lett. **50**, 433 (1987).
[37] M. Kawasaki and Y. Kawaguchi, Appl. Phys. Lett. **62**, 3099 (1993).
[38] R. Robertson and M. Rossi, J. Chem. Phys. **91**, 5037 (1989).
[39] K. Tachibana, Mater. Sci. Eng. B **17**, 68 (1993).
[40] F. Kampas and R. Griffith, J. Appl. Phys. **52**, 1285 (1981).
[41] C. Bohm and J. Perrin, J. Phys. D **24**, 865 (1991).
[42] J. Perrin, P. Cabarrocas, B. Allain, and J. Friedt, Jpn. J. Appl. Phys. **27**, 2041 (1988).
[43] V. A. Godyak and A. S. Khanneh, IEEE Trans. Plasma Sci. **PS-14**, 112 (1986).
[44] Hydrocarbon contamination is likely due to exposure to atmosphere prior to FTIR analysis.
[45] A more complete analysis of the OH reactivity is given elsewhere. K. H. A. Bogart, J. P. Cushing, and E. R. Fisher, Chem. Phys. Lett. (accepted).